

UC Irvine

UC Irvine Previously Published Works

Title

Algorithm for the Estimation of Ultrawideband Scattering by a Target for Automotive Applications

Permalink

<https://escholarship.org/uc/item/940292rs>

Authors

Passalacqua, G
Albani, M
Capolino, F
et al.

Publication Date

2006

DOI

10.1109/APS.2006.1711606

Copyright Information

This work is made available under the terms of a Creative Commons Attribution License, available at <https://creativecommons.org/licenses/by/4.0/>

Peer reviewed

Algorithm for the Estimation of Ultrawideband Scattering by a Target for Automotive Applications

G. Passalacqua⁽¹⁾, M. Albani^{(1)*}, F. Capolino⁽¹⁾, R. Gardelli⁽³⁾,
M. Branciforte⁽²⁾ and R. Martorana⁽²⁾

(1) Dept. of Information Engineering, University of Siena, Siena, Italy

(2) STMicroelectronics, Catania, Italy

(3) DFMTFA, University of Messina, Messina, Italy

I. INTRODUCTION

The interest in the development of radar technologies in automotive systems to increase the drivers' safety standard has motivated our research on a simulator to predict the ultrawideband (UWB) scattering by a generic target discretized with a triangular mesh (Fig. 1(a) is a CAD image of a car). Radar systems that employ UWB short pulses (Fig. 1(b) is a typical pulse $s_{TX}(t)$ used in automotive) permit high space resolution and an efficient transmission of electromagnetic energy [1].

In the frequency domain, the physical-optics (PO) method is one of most used techniques of high frequency analysis to study the interaction between the electromagnetic waves and large (in terms of wavelength) targets and it does not require special treatment of shadow boundaries of rays species. In UWB systems it is convenient to use the PO in time domain (TD) [2] [3]. The TDPO considerably reduces the computation time of simulations involving a large span of frequencies. Here, we present three different algorithms called *Space Quantization*, *Planar Wavefront*, and *Spherical Wavefront* to predict the field scattered by a target.

In Section II of this summary, there is a short introduction to the TDPO method, followed by the description of the three developed algorithms. In Section III some numerical results are presented including a comparison of the performances of the three algorithms.

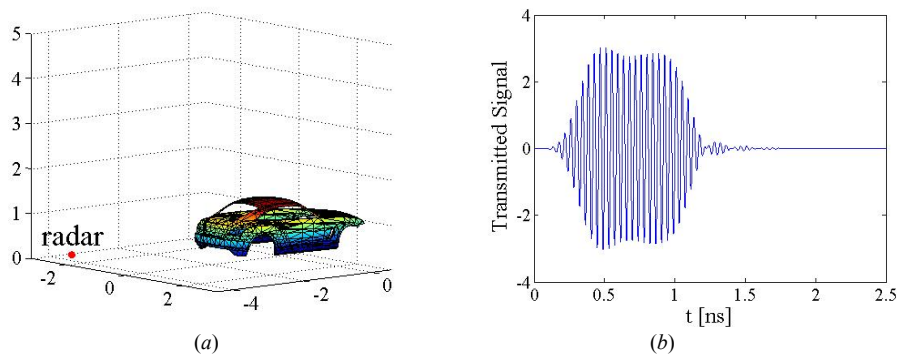


Fig. 1. Typical scenario. (a) sensor and target arrangement, (b) UWB incident signal waveform $s_{TX}(t)$ at the antenna terminals

II. FORMULATION

Any arbitrary target is assumed to be represented in terms of triangular facets, thus the entire response is calculated as superposition of responses by many triangular flat plates. Here we present the derivation of the radar response of a single triangular plate which represents the basic block in our computational algorithm.

Consider a triangular plate with vertices at P_1, P_2, P_3 (Fig. 2(a)) illuminated by a radar antenna at P' . The incident electric field at a point Q on the triangle surface is

$$\mathbf{e}^{inc}(Q, t) = s_{TX} \left(t - \frac{R}{c} \right) \frac{1}{4\pi R} \mathbf{f}(\hat{\mathbf{R}}), \quad (1)$$

in which the radiation vector \mathbf{f} is related to the antenna gain G by $|\mathbf{f}(\hat{\mathbf{R}})|^2 = 8\pi\eta_0 G(\hat{\mathbf{R}})$. Without loss of generality, we assume the radar antenna to be linearly polarized and non dispersive (in the band of interest), consequently \mathbf{f} and G are independent of time/frequency. The current on the triangle surface is calculated under PO approximation as $\mathbf{j}(Q, t) = 2\hat{\mathbf{n}} \times \mathbf{h}^{inc}(Q, t)$, where $\mathbf{h}^{inc}(Q, t)$ is the incident magnetic field. Then, the field backscattered by the triangle back to the antenna location P' is calculated under the PO approximation, in far field regime, as

$$\mathbf{e}^s(P', t) = \mu_0 \iint_{triangle} \frac{1}{4\pi R} (\mathbf{1} - \hat{\mathbf{R}}\hat{\mathbf{R}}) \cdot \frac{\partial}{\partial t} \mathbf{j} \left(Q, t - \frac{R}{c} \right) dS, \quad (2)$$

leading to a received echo signal $s_{RX}(t) = \frac{1}{4\mu_0} \mathbf{f}(\hat{\mathbf{R}}) \cdot \int_{-\infty}^t \mathbf{e}^s(P', \tau) d\tau$. After substitution we obtain

$$s_{RX}(t) = - \iint_{triangle} \frac{\hat{\mathbf{n}} \cdot \hat{\mathbf{R}}}{4\pi R^2} G(\hat{\mathbf{R}}) s_{TX} \left(t - 2\frac{R}{c} \right) dS, \quad (3)$$

which expresses the echo signal in terms of the geometrical arrangement. Equation (3) is numerically calculated resorting to three different schemes, that are detailed in the following, each one has been found efficient for different triangle sizes.

A. SPACE QUANTIZATION

The *Space Quantization* method computes the radiation integral (3) by discretizing the target surface with a triangular mesh provided by the CAD 3D Studio. Based on the physical characteristics of the object and the electromagnetic features of the incident field and starting from the triangular mesh of the surface, we calculate the response contribution of each triangle as the sum of the fields reflected by the *sub-triangles* obtained from a further sub-division. In particular, if a sub-triangle has sides shorter than a quarter of the smaller wavelength of the transmitted signal ($D_{max} < \lambda_{min}/4$), it is possible to approximate the PO current as constant on the whole sub-triangle and equal to the value at the barycenter of the element. The same approximation is used in the evaluation of the scattered field. Under these hypothesis (3) becomes

$$s_{RX}(t) \approx - \sum_i \frac{\hat{\mathbf{n}} \cdot \hat{\mathbf{R}}_i}{4\pi R_i^2} G(\hat{\mathbf{R}}_i) s_{TX} \left(t - 2\frac{R_i}{c} \right) A_i, \quad (4)$$

where R_i is the distance between the barycenter of the sub-triangle and the source, and A_i is the area of the i -th sub-triangle.

B. PLANAR WAVEFRONT

In this case the incident signal is assumed to be impulsive

$$s_{TX}(t) = \delta(t). \quad (5)$$

We suppose to subdivide a triangular plate in smaller sub-triangles (larger than in the previous case) with size such that the radar antenna is still in their far field zone ($D_{max} < \sqrt{r\lambda_{min}/2}$). Combining (3) and (5) we obtain the impulsive response of each sub-triangle

$$h_{RX}(t) = - \iint_{triangle} \frac{\hat{\mathbf{n}} \cdot \hat{\mathbf{R}}}{4\pi R^2} G(\hat{\mathbf{R}}) \delta \left(t - 2\frac{R}{c} \right) dS \approx - \frac{\hat{\mathbf{n}} \cdot \hat{\mathbf{R}}_0}{4\pi R_0^2} G(\hat{\mathbf{R}}_0) \iint_{triangle} \delta \left(t - 2\frac{R_0 + \hat{\mathbf{R}}_0 \cdot \mathbf{r}}{c} \right) dS. \quad (6)$$

Assuming the sub-triangle surface in the x - y plane (x orthogonal and y parallel to the intersection between the sub-triangle and the propagating wavefront), we have

$$\hat{\mathbf{R}}_0 \cdot \mathbf{r} = \hat{\mathbf{R}}_0 \cdot \hat{\mathbf{x}}x = \sqrt{1 - (\hat{\mathbf{R}}_0 \cdot \hat{\mathbf{n}})^2} x, \quad \text{and} \quad \delta\left(t - \frac{2}{c}\left(R_0 + \sqrt{1 - (\hat{\mathbf{R}}_0 \cdot \hat{\mathbf{n}})^2} x\right)\right) =$$

$$= \frac{c}{2\sqrt{1 - (\hat{\mathbf{R}}_0 \cdot \hat{\mathbf{n}})^2}} \delta\left(x - \left(R_0 - \frac{ct}{2}\right) / \sqrt{1 - (\hat{\mathbf{R}}_0 \cdot \hat{\mathbf{n}})^2}\right). \quad \text{The Dirac delta permits to}$$

evaluate the integral in x in closed form, the evaluation of the remaining integral in y gives the segment length of the intersection between wavefront and sub-triangle shown in Fig. 2(a) between Q_1 and Q_3 , leading to the target impulsive response

$$h_{RX}(t) = -\frac{c}{8\pi R_0^2} \frac{\hat{\mathbf{n}} \cdot \hat{\mathbf{R}}_0}{\sqrt{1 - (\hat{\mathbf{n}} \cdot \hat{\mathbf{R}}_0)^2}} G(\hat{\mathbf{R}}_0) \ell(t). \quad (7)$$

The UWB received signal is equal to the convolution between the transmitted waveform signal and the impulsive response $s_{RX}(t) = s_{TX}(t) \otimes h_{RX}(t)$, which, for short pulse excitation, involves only a few nonvanishing terms thus being very efficient.

C. SPHERICAL WAVEFRONT

We evaluate here the impulsive response of a triangular plate to an incident field with spherical wavefront to avoid the subdivision in small sub-triangles. Without loss of generality we assume the antenna to have a constant gain in the angular range occupied by the plate, then (3) becomes

$$h_{RX}(t) = -G(\hat{\mathbf{R}}_0) \iint_{\text{triangolo}} \frac{\hat{\mathbf{n}} \cdot \hat{\mathbf{R}}}{4\pi R^2} \delta\left(t - \frac{2R}{c}\right) dS. \quad (8)$$

The intersection between the incident spherical wavefront and the plane containing the triangle is a circumference with center C and radius $\sqrt{\left(\frac{ct}{2}\right)^2 - R_C^2}$, with $|P' - C| = R_C$

(In Fig. 2(b) the triangular is plate illuminated by an incident field with spherical wavefront). Mapping the integral in polar coordinates ρ, ϕ , we have

$$\delta\left(t - \frac{2R}{c}\right) = \delta\left(t - 2\frac{\sqrt{\rho^2 + R_C^2}}{c}\right) = \frac{c^2 t}{4\sqrt{\left(\frac{ct}{2}\right)^2 - R_C^2}} \delta\left(\rho - \sqrt{\left(\frac{ct}{2}\right)^2 - R_C^2}\right) \quad \text{and the Dirac}$$

delta permits to evaluate in closed form the ρ -integral. The ϕ -integral is evaluated as

the length of the circumference arcs inside the triangle $\ell_{arc}(t) = \sqrt{R_C^2 - \left(\frac{ct}{2}\right)^2} \alpha_{arc}(t)$,

with $\alpha_{arc}(t)$ the angular width of arcs. The impulsive response (8) is thus reduced to

$$h_{RX}(t) = -G(\hat{\mathbf{R}}_0) \frac{R_C}{2\pi c t^2} \alpha_{arc}(t) \quad (9)$$

and the received signal is evaluated as $s_{RX}(t) = s_{TX}(t) \otimes h_{RX}(t)$.

III. NUMERICAL RESULTS

Figure 3 shows the computation time of the three methods for an equilateral triangular plate with varying size. The sub-triangle subdivision is automatic in the first two methods depending on some threshold parameters not discussed here. Note that the

fastest one is the Space Quantization for small triangles and the Spherical Wavefront method for large triangles. The Planar Wavefront is a good compromise.

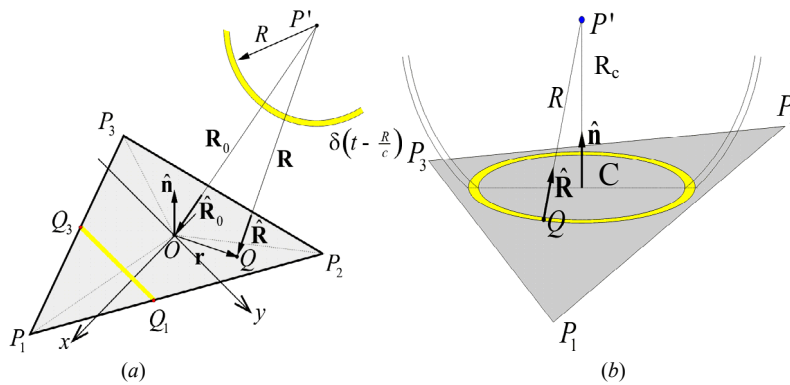


Figure 2. A triangular plate of the mesh.

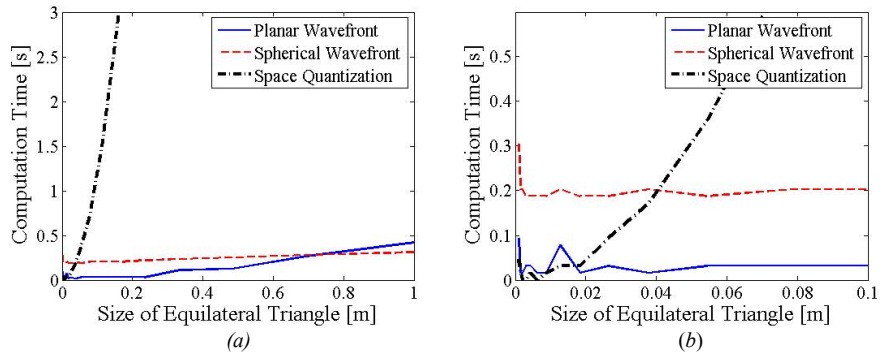


Fig. 3. Computation Time versus triangle size ranging (a) 1mm – 1m and (b) 1mm – 10cm (zoom)

The car target is illuminated by the typical incident pulse waveform shown in Fig. 1(b) and received signal is evaluated at the radar location, shown in Fig. 4(b) using the TDPO *Planar Wavefront* method. According to the TDPO, only the illuminated facets shown in Fig. 4(a) are considered. The other two methods provide the same accuracy but the *Planar Wavefront* method is the most effective one for the given mesh and geometry.

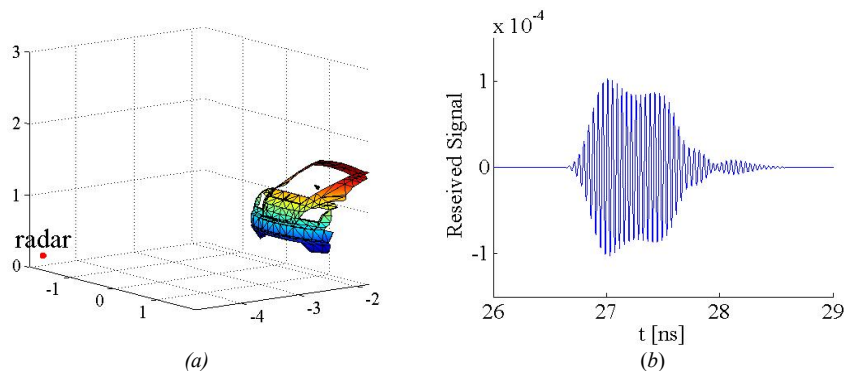


Fig. 4. Simulation scenario. (a) Visible facets by the radar, (b) Received signal $s_{rx}(t)$.

REFERENCES

- [1] J. D. Taylor, *Introduction to Ultra-Wideband Radar System*, CRC Press, (1995).
- [2] En-Y. Sun and W. V. T. Rusch, "Time-Domain Physical-Optics", *IEEE Trans Antennas Propagat.*, Vol. 42, Jan. 1994.
- [3] C. E. Baum, "Transient Scattering Length and Cross Section", *Interaction Note 484*, April 1991.